Meta-GGA Exchange-Correlation Free Energy Density Functional to Increase the Accuracy of Warm-Dense-Matter Simulations

V. V. Karasiev, D. I. Mihaylov, and S. X. Hu

Laboratory for Laser Energetics, University of Rochester

High-energy-density physics includes a complicated warm-dense-matter (WDM) domain of state conditions that is characterized by elevated temperatures (from few to hundreds of eV) and pressures to 1 Mbar or greater. Accurate knowledge of equation of state, transport, and optical properties describing possible phase transitions (e.g., insulator-to-metal transition) across a warm dense regime plays an important role in planetary science, astrophysics, and inertial confinement fusion.[1–6] Currently, the vast majority of density-functional-theory (DFT) simulations of WDM and high-energy-density plasmas use the zero-temperature (ground-state) exchange-correlation (XC) functionals without explicit temperature dependence, which were developed by the condensed-matter physics and quantum chemistry communities, leading to neglect of thermal XC effects and degraded accuracy of predictions. The use of a ground-state XC functional is justified only at low electronic temperatures not exceeding a few tenths of the Fermi temperature or in the high-temperature limit when the XC contribution to the total free energy is negligible.[7–10] Recent development of the temperature-dependent Karasiev–Sjostrom–Dufty–Trickey (KSDT)[11] local-density approximation (LDA) (see Ref. 12 for the corrected set of parameters corrKSDT), the generalized gradient approximation (GGA)–type XC functional "KDT16" (Ref. 12), and the thermal hybrid KDT0[13] have shown that thermal XC effects are very important to increasing the accuracy of simulations at extreme conditions and improving agreement with experimental measurements as compared to the standard zero-temperature Perdew–Burke–Ernzerhof (PBE)[14] calculations. The way to improve overall accuracy of the thermal GGA XC functional is to use the next rung approximation at zero temperature and construct thermally extended meta-GGA XC.

In this work, we address this problem by developing a thermalization framework for XC functionals at the meta-GGA level of refinement and realization of a simple scheme via universal thermal XC additive correction at the GGA level of theory, which is applied to an accurate at low-T, ground-state meta-GGA XC. Thermal correction is applied to the ground-state deorbitalized, strongly constrained, and appropriately normed semilocal density functional (SCANL)[15–18]—to date, one of the most-accurate meta-GGA XC functionals, which, for example, is capable of accurately describing the liquid–liquid insulator-to-metal transition of warm dense hydrogen.[3] The resulting thermal meta-GGA XC functional, referred to here as T-SCAN-L, inherits the precision of the ground-state meta-GGA SCAN-L at low T, and most of the thermal XC effects are captured at the GGA level of theory, providing overall a much higher accuracy across the temperature regimes spanned by the WDM domain.

With increasing temperature, the electron density approaches the slowly varying regime. The KDT16 GGA functional, by construction, recovers the finite-T gradient expansion. Thermal XC corrections beyond the GGA level are expected to be small; therefore, in the following we propose a simple perturbative-like self-consistent approach via a universal thermal additive correction treated self-consistently, similar to the idea used in Ref. 19 to construct GGA XC with additive thermal LDA correction. The KDT16 XC free energy in the zero-T limit reduces to the ground-state PBE by construction:

$$\lim_{T\to 0} \mathcal{F}_{\mathrm{xc}}^{\mathrm{KDT16}}\left[n,T\right] \approx E_{\mathrm{xc}}^{\mathrm{PBE}}\left[n\right], \tag{1}$$

a choice driven by popularity of the PBE functional and by availability of pseudo-potentials and projector augmented wave (PAW) data sets generated by using the PBE XC. Given the quality of SCAN-L functional at zero temperature, we propose a simple temperature-dependent meta-GGA

$$\mathcal{F}_{\mathrm{xc}}^{\text{meta-GGA}}[n,T] = E_{\mathrm{xc}}^{\text{meta-GGA}}[n] + \Delta\mathcal{F}_{\mathrm{xc}}^{\mathrm{GGA}}[n,T], \tag{2}$$

with the additive thermal correction defined as follows:

$$\Delta\mathcal{F}_{\mathrm{xc}}^{\mathrm{GGA}}[n,T] := \mathcal{F}_{\mathrm{xc}}^{\mathrm{KDT16}}[n,T] - E_{\mathrm{xc}}^{\mathrm{PBE}}[n] \tag{3}$$

and meta-GGA = SCAN-L. An explicit functional form defined by Eqs. (2) and (3) is used in standard fully self-consistent DFT calculations with local XC potential calculated as a functional derivative of $\mathcal{F}_{\mathrm{xc}}^{\text{meta-GGA}}[n,T]$ with respect to electron density n.

Ab initio molecular dynamics (AIMD) simulations that demonstrate the superior accuracy of the new T-SCAN-L meta-GGA functional are for dense helium. Figure 1 compares relative errors for total pressures obtained from DFT simulations with four XC functionals and high-quality path-integral Monte Carlo (PIMC). PIMC is an efficient *first-principles* simulation technique for quantum systems at finite temperature that accurately takes into account the Coulombic interaction between electrons using pair-density matrices, so it therefore can be used to benchmark approximate XC density functionals at elevated temperatures.[7] Both ground-state functionals (PBE and SCAN-L) systematically overestimate the total pressure: the relative error with respect to the reference PIMC data is between 4.2% and 5.8% at T = 10.77 eV. In contrast, the T-SCAN-L total pressures are in excellent agreement with the PIMC values, demonstrating unprecedented accuracy between 0.05% and 0.35% for this range of densities. Relative differences between the KDT16 and PIMC values are larger as compared to the T-SCAN-L values and range from 0.4% to 1.4%. These comparisons show that T-SCAN-L calculations can improve the DFT simulation accuracy for He at these warm dense conditions by a factor of ~3 to 10 over the widely used XC functionals (PBE, SCANL, and KDT16). This clearly demonstrates that the T-SCAN-L meta-GGA functional can accurately capture combined XC thermal and nonhomogeneity effects. When temperature increases to 21.54 eV, the relative error of the ground-state functionals reduces to the range between 1.3% and 3.6% (because the XC contribution becomes less important as compared to the noninteracting free-energy term at high T), while the relative difference between T-SCAN-L and PIMC values is still less than ~1%.

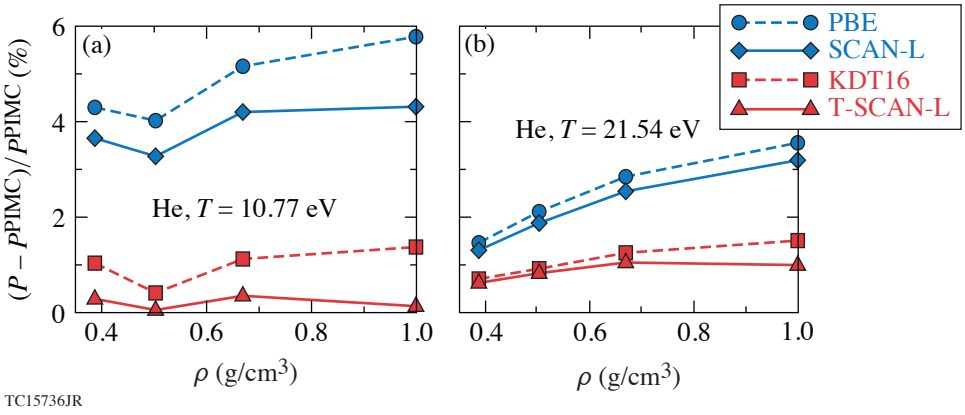

Figure 1
The relative error of total pressure from AIMD simulations of warm dense He using PBE, SCAL-L, KDT16, and T-SCAN-L XC functionals calculated with respect to the reference PIMC results and shown as a function of material density for two temperatures.

The simplest thermalization scheme, which uses a universal additive thermal correction and a perturbative-like self-consistent approach, has been implemented, leading to thermal T-SCAN-L functional. The nonempirical T-SCAN-L meta-GGA density functional takes into account combined thermal and nonhomogeneity effects at the meta-GGA level, providing a significantly higher accuracy for DFT to better predict material properties in the WDM regime, as compared to the thermal KDT16, and to the ground-state PBE and SCAN-L XC functionals. In the zero-temperature limit, T-SCAN-L reduces to its ground-state counterpart, therefore preserving the SCAN-L meta-GGA level of accuracy at low T.

This material is based upon work supported by the Department of Energy National Nuclear Security Administration under Award Number DE-NA0003856 and U.S. National Science Foundation PHY Grant No. 1802964. This research used resources of the National Energy Research Scientific Computing Center, a DOE Office of Science User Facility supported by the Office of Science of the U.S. Department of Energy under Contract No. DE-AC02-05CH11231.

1. J. J. Fortney and N. Nettelmann, Space Sci. Rev. **152**, 423 (2010).
2. W. Lorenzen, B. Holst, and R. Redmer, Phys. Rev. B **84**, 235109 (2011).
3. J. Hinz *et al*., Phys. Rev. Research **2**, 032065(R) (2020).
4. C. A. Iglesias, F. J. Rogers, and D. Saumon, Astrophys. J. Lett. **569**, L111 (2002).
5. S. X. Hu *et al*., Phys. Plasmas **22**, 056304 (2015).
6. V. V Karasiev and S. X. Hu, Phys. Rev. E **103**, 033202 (2021).
7. V. V. Karasiev, L. Calderín, and S. B. Trickey, Phys. Rev. E **93**, 063207 (2016).
8. V. V. Karasiev, S. B. Trickey, and J. W. Dufty, Phys. Rev. B **99**, 195134 (2019).
9. K. Ramakrishna, T. Dornheim, and J. Vorberger, Phys. Rev. B **101**, 195129 (2020).
10. M. Bonitz *et al*., Phys. Plasmas **27**, 042710 (2020).
11. V. V. Karasiev *et al*., Phys. Rev. Lett. **112**, 076403 (2014).
12. V. V. Karasiev, J. W. Dufty, and S. B. Trickey, Phys. Rev. Lett. **120**, 076401 (2018).
13. D. I. Mihaylov, V. V. Karasiev, and S. X. Hu, Phys. Rev. B **101**, 245141 (2020).
14. J. P. Perdew, K. Burke, and M. Ernzerhof, Phys. Rev. Lett. **77**, 3865 (1996); **78**, 1396(E) (1997).
15. J. Sun, A. Ruzsinszky, and J. P. Perdew, Phys. Rev. Lett. **115**, 036402 (2015).
16. H. Peng *et al*., Phys. Rev. X **6**, 041005 (2016).
17. D. Mejia-Rodriguez and S. B. Trickey, Phys. Rev. A **96**, 052512 (2017).
18. D. Mejia-Rodriguez and S. B. Trickey, Phys. Rev. B **98**, 115161 (2018).
19. T. Sjostrom and J. Daligault, Phys. Rev. B **90**, 155109 (2014).